Morning transition case between the land and the sea breeze regimes

Maria A. Jiménez[a,b,*], Gemma Simó[b], Burkhard Wrenger[c], Maja Telisman-Prtenjak[d], Jose A. Guijarro[e], Joan Cuxart[b]

[a] *Institut Mediterrani d'Estudis Avançats (UIB-CSIC), Esporles, Illes Balears, Spain*
[b] *Universitat de les Illes Balears, Palma de Mallorca, Illes Balears, Spain*
[c] *University of Applied Sciences Ostwestfalen-Lippe, Höxter, Germany*
[d] *Faculty of Sciences, University of Zagreb, Zagreb, Croatia*
[e] *Delegació territorial Illes Balears, Agencia Estatal de Meteorologia (AEMET), Palma de Mallorca, Illes Balears, Spain*

Abstract

An experimental field campaign took place in September 2013 near the coastline in the southeastern Campos basin in the island of Mallorca to characterize experimentally the transition between the sea and land breezes and to further study the successful cases with the corresponding high-resolution numerical simulations. Favorable weather conditions were only found for one episode that comprised a well formed nocturnal land breeze, followed by the morning transition to sea-breeze until noon the next day, when incoming clouds switched off the breeze regime.

To analyse this transition between land and sea breezes the official network of stations is used, supplemented by a portable station close to the shore and soundings of temperature (taken by a captive balloon and remotely controlled multicopter). These data are used to check the goodness of the corresponding simulation at a horizontal resolution of 1 km. Model and observations see similarly both regimes and the transition, showing some

*Corresponding author: Maria A. Jiménez. Grup de Meteorologia, Dept. Física, Universitat de les Illes Balears, Carret. Valldemossa km 7.5, 07122-Palma de Mallorca (Illes Balears) Spain. Telephone: +34 971259542.

Email addresses: mantonia.jimenez@uib.cat (Maria A. Jiménez), gemma.simo@uib.es (Gemma Simó), burkhard.wrenger@hs-owl.de (Burkhard Wrenger), telisman@gfz.hr (Maja Telisman-Prtenjak), jguijarrop@aemet.es (Jose A. Guijarro), joan.cuxart@uib.cat (Joan Cuxart)

differences in the timing and the details in the surface layer. This transient event is analyzed in terms of phases, going consecutively through land-breeze, phase previous to the sea breeze, when land heating starts but it is still colder than the sea, the preparatory phase when the land becomes warmer than the sea, and the development phase when the breeze front progresses inland.

Keywords: field campaign, land-breeze, mesoscale modelling, morning transition, sea-breeze

1. Introduction

The Atmospheric Boundary Layer (ABL), which is the layer of air directly affected by the presence of the underlying surface, can have different regimes, depending on the large-scale forcings. When the general winds are weak and the cloudiness is low enough to allow the surface net radiation to have a diurnal cycle, the ABL shows a characteristic evolution, with a Convective Boundary Layer (CBL) in the daytime and a stably stratified boundary layer (SBL) at night, with the two corresponding morning and evening transition events in between (Garratt, 1992).

Whereas the CBL is essentially a turbulence driven regime by surface heating, the SBL over homogeneous terrain is mainly controlled by the surface radiative cooling, that can be transported upwards if there is turbulence generated by the wind shear. The transitions are governed by the establishment of a thermal surface inversion in the evening and by the destruction of the inversion in the morning. These transitions are currently a subject of study of deep interest due to their incomplete characterization so far for several reasons: (1) the difficulties to measure the surface energy budget and the relative importance of the terms (Cuxart et al., 2015), (2) the similarity theories that may not be of application since the heat fluxes and the wind are nearly zero, and there is still not a widely accepted similarity theory to describe the surface layer in these conditions (Lapworth (2003); Lapworth (2006)), (3) the definition and quantification of the boundary-layer depth (Lothon et al., 2014), (4) the fact that turbulence may be intermittent and anisotropic (Sun et al., 2012), (5) the temporal evolution of the surface fluxes and their dependence on the heterogeneity of the surface (Nadeau et al., 2011), (6) the processes in complex terrain regions that make a more complicated picture of the dynamics of the morning transition (Lenschow et al., 1979). In heterogeneous terrain, the slope winds generated by hor-

izontal thermal differences interact with other flows and modify the ABL state. Typical cases are the slope and the valley flows that increase the wind shear at lower levels and enhance mixing close to the surface (Whiteman, 2000), or the sea and land breezes, that may even change the turbulence regime, for instance making it thermally unstable at night over the sea by the coast (Cuxart et al., 2007).

The Land Breeze (LB) and the Sea Breeze (SB) have already been studied numerically by some of the authors of this study (Cuxart et al. (2007); Cuxart et al. (2014), from now on CJTG14) for the island of Mallorca, using data from the operational network for validation of the model results. The regimes are strongly modulated by the presence of moderate terrain slopes that contribute to the establishment of LB and SB and the topographical features of the three main basins of the island (Figure 1). At night downslope flows converge to the center of the basins and are expelled towards the sea enhanced by the LB, whereas in the daytime, SBs from the different basins tend to converge at the center of the island (Ramis and Romero, 1995). In CJTG14 a deeper analysis was performed for the SB in the Campos basin, at the SE of the island. The budgets of momentum, temperature and turbulence extracted from the model were used and a proposition of phases of the evolution of the SB was stated.

In this work, the focus is put on the morning transition (MT), whereas the previous efforts where devoted to the LB and SB separately. Here the coastal area is the zone of study, instead for those studies the analysis was performed for the central part of the Campos basin, exploring the interaction of the breeze and the slope flows. As before, we dispose of numerical simulations and the operational network of the Spanish Weather Services, but an additional experimental display is set, operating a supplemental weather station close to the coastline, and a tethered balloon and a multicopter drone to provide profiles for the lowest hectometers of the atmosphere. This configuration has allowed to characterize a MT case between a LB and a SB regimes, both experimentally and numerically, progressing towards a more complete picture of the daily cycle of this regime.

The paper is organized as follows: after the Introduction, Section 2 describes the typical LB and SB regimes for the site of interest, the particular case that is studied, the available data and a summary of the model results. Section 3 expands on the description of the model outputs and how they compare to the available observational data. Section 4 makes the interpretation of the MT in terms of the SB phases introduced in CJTG14 and supplements

it with the analysis of the LB which was not analyzed in that work. Finally Section 5 makes a technical sensitivity study showing how a minor issue in the turbulence parameterization (the minimum value allowed for the turbulence kinetic energy) may change the surface layer profiles significantly and even some details of the LB/SB regime.

2. The studied case and the model setup

2.1. The LB/SB regime and its occurrence in Mallorca

The diurnal variation of the land-sea differential heating produces a cross-shore pressure gradient and an onshore/offshore wind is generated during the day/night (SB/LB) (Atkinson, 1981). The general knowledge about the main features of the SB show that a maximum wind speed is formed below 800 m (above ground level, agl) of about 5 m s^{-1} (Bechtold et al., 1991) just after the maximum insolation (between 1500-1700 UTC for the island of Mallorca, CJTG14). Most of the studies related to the SB are mainly focused on the mature phase, being worth mentioning the study of the establishment of the SB/LB, their return currents at higher levels of Johnson and O'Brien (1973) in the central Oregon coast (USA), the impact on the modelled surface features to properly capture the onset of SB by Miao et al. (2003) or their interactions with the larger-scale wind (Bora, Telisman-Prtenjak et al. (2010)).

The climatological analysis of Azorin-Molina and Chen (2009) of the surface observations in the easterly Iberian Peninsula shows that the initiation of the SB depends on the strength of the LB and also on the direction and intensity of the synoptical wind. Panchal (1993) indicates that the initiation of the SB also depends on the features of the previous SB, besides the thermal difference between land and sea.

Mallorca, an island located in the Western Mediterranean Sea, 200 km to the east of the Iberian Peninsula, has two mountain ranges at the north and east together with an elevated area in the central part and in between there are three well-defined basins with different topographical characteristics (see Figure 1). The SBs formed in these basins converge at the center of the island, where an updraft area is found (Ramis and Alonso, 1998), prone to storm developments if unstable conditions are found at higher levels and there is enough moisture between 850 hPa and 700 hPa to support further development (as it is reported in south-eastern Italy in Nelci et al. (2015) or in Istria, Croatia, in Poljak et al. (2014)). The SB regime in Mallorca

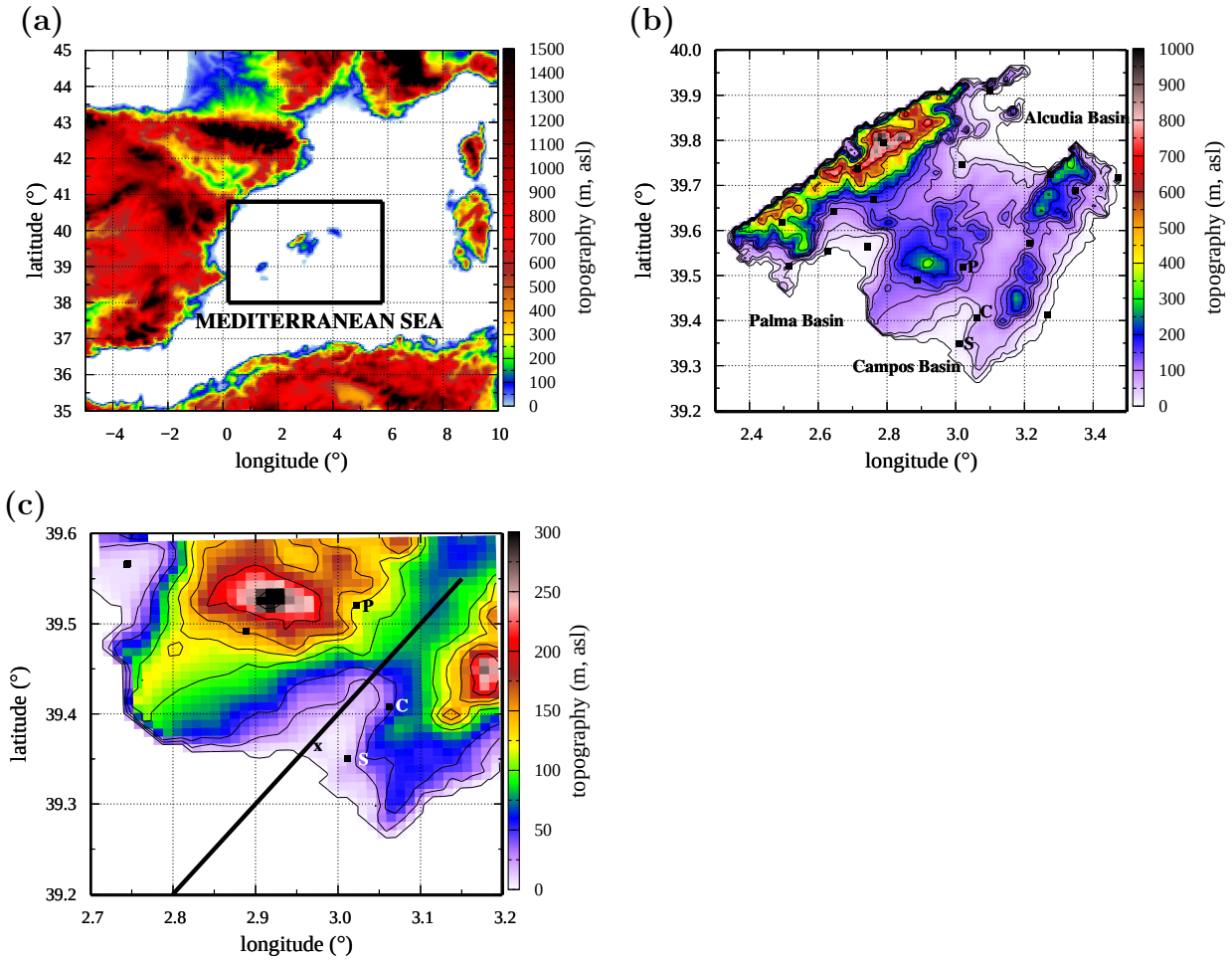

Figure 1: **(a)** Location of the Balearic Islands in the Western Mediterranean Sea. The black box indicates the limits of the outer domain of the simulation. The topography of Mallorca (inner domain of the simulation) is shown in **(b)** and in **(c)** a zoom in the Campos basin. The locations of the surface weather stations from the Spanish Meteorological Service (AEMET) are indicated with a black square and those placed in the Campos basin are labelled as: *C* Campos; *S* Ses Salines and *P* Porreres. The central parts of the three main basins are coloured in purple, and their names are indicated in **(b)** over the sea, in front of the coastline. The cross in **(c)** indicates the place where the MSB13 experimental field campaign took place (tethered balloon, multicopter and surface observations). The black line indicates the vertical cross-section showed in Figures 5 and 8.

was first studied by Jansà and Jaume (1946) and later Ramis and Romero (1995) made an idealized numerical study that showed the importance of the surface conditions, specially soil moisture, in the development of the SB.

The recent numerical study of CJTG14 has suggested to define different consecutive phases for the SB (previous, preparatory, development, mature and decaying) with respect to the different ABL regimes over land and over sea and with a detailed description of the mature phase of the SB. On the other hand, previous studies (Jiménez et al. (2006); Cuxart et al. (2007)) were devoted to studying the LB regime. In this work, the processes that take place during the transition between LB and SB regimes are further studied, now aided by specific observational evidence, gathered during an experimental campaign in 2013.

2.2. The Mallorca Sea Breeze 2013 (MSB13) experimental field campaign

In September 2013 a 5-day measurement campaign took place at the site of Ses Covetes (indicated with a cross in Figure 1) centrally located in the Campos basin, 500 m inland. The SB intensity at that time of the year allows to operate safely tethered balloons or drones, compared to the stronger and very turbulent wind conditions found in July or early August. During the campaign, Mallorca was under the influence of a high-pressure system on the Atlantic Ocean, centered to the west of the Iberian Peninsula. Synoptic forcing and cold air at upper levels generated clouds and storms and prevented the SB regime to develop until September 20, when weak winds allowed the establishment of a well defined LB at night and a good MT afterwards, leading to a SB development that was later interrupted by clouds and rain following a convective development (as in Azorin-Molina et al. (2014)). However the interval between 0400 and 1100 UTC was an optimal case of MT between LB and SB.

The Campos basin has a number of automated weather stations belonging to AEMET (Spanish weather Service) of which we use Ses Salines, Campos and Porreres, located respectively at 3 km, 10 km and 25 km inland from Ses Covetes. A supplementary station of the University of the Balearic Islands (UIB) was installed at Ses Covetes which sampled at a rate of 1 Hz wind, temperature and relative humidity at 2 m agl. A tethered balloon developed by UIB and the Ostwestfalen-Lippe (OWL) Hochschule was operated when possible and provided profiles of temperature at a rate of 1 Hz, that were later post-processed to give profiles with a vertical resolution of 1 m. A similar equipment was aboard a remotely controlled OWL multicopter. The

balloon and multicopter sensors were calibrated with the UIB station and corrections have been made to remove the effects of solar radiation during daytime operation in profiling.

2.3. Surface layer observations of the analyzed morning transition

As mentioned above, the MT between LB and SB of September 20, 2013 is taken for analysis. The surface observations in the Campos basin are shown in Figure 2 (in dots) for the AEMET surface stations (Campos, Ses Salines and Porreres) together with the ones measured in Ses Covetes (see locations in Figure 1c).

During the night-time and until two hours after sunrise, the wind is weak (about 1 m s^{-1}) in all the surface stations of the Campos basin. Mechanical anemometers of the AEMET network have threshold values of around 1 m s^{-1} and under these conditions the wind direction remains fix. Therefore, their measurements are to be taken with caution during that period. On the contrary, since the UIB wind sensor at Ses Covetes is a 2D sonic anemometer, it does not have a low threshold value and it is able to measure the changes in the wind direction for weak wind speeds. The observed wind in Ses Covetes is close to zero most of the night-time and therefore the wind direction is fluctuating. It is important to mention that for the AEMET network the wind is observed at 10 m agl whereas observations in Ses Covetes are taken at 2 m agl, closer to the surface and within the surface layer inversion that, under these conditions, is decoupled from the layer aloft (Cuxart and Jiménez, 2007). Therefore, the observed wind in Ses Covetes is strongly influenced by the local effects, such as local slopes or surface heterogeneities (Martínez et al., 2010). During night, observations in Ses Covetes indicate predominance of weak winds from E and NE, the usual direction of LB in this part of the basin. About two hours after sunrise, the wind speed progressively increases while it turns towards the S-SW direction in all the surface stations, corresponding to the SB in this region.

Observations along the Campos basin show that the temperatures are similar for all the stations in the LB phase (before sunrise, at about 0600 UTC) although the coldest temperatures are found near the coastline (in Ses Covetes) and decrease towards the inland direction. This might be related to the fact that measurements in Ses Covetes are taken in the lower part of the Campos basin, where cold air accumulates as it is found in the Duero basin (Martínez et al., 2010). After sunrise, the temperature becomes homogeneous for all stations in the basin, increasing until the SB starts blowing, near

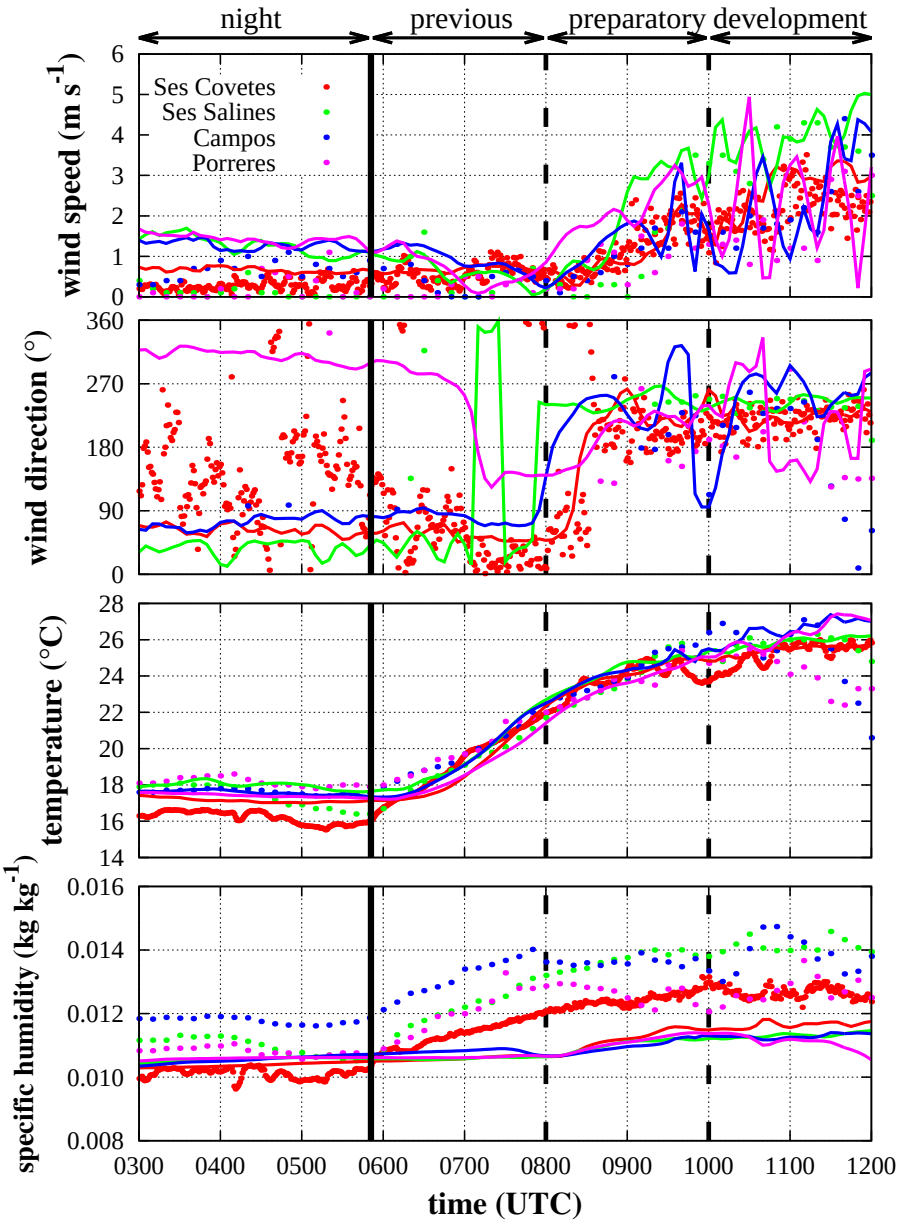

Figure 2: Observed (dots) and modelled (lines) time series during the different phases of the morning transition of the SB (names indicated in the top of the plot) reported on 20 September 2013 during the MSB13 experimental field campaign for: **(a)** wind speed (in m s^{-1}), **(b)** wind direction (in °, north is 0°), **(c)** temperature (in °C) and **(d)** specific humidity (in kg kg^{-1}). The wind is measured at 10 m agl and the temperature and humidity at 2 m agl in the AEMET surface weather stations and in the MSB13 site (Ses Covetes) all magnitudes are at 2 m agl. The black vertical line indicates the sunrise time and the dotted ones the different phases during the morning transition.

1000 UTC that day. Afterwards, warming stops and the temperature stays approximately homogeneous and constant in all the stations in the basin except for the most inland surface weather stations (Campos and Porreres) because they are influenced by the presence of clouds.

The specific humidity is nearly constant during night-time, with the wettest locations in the center of the basin. This pattern is kept over the MT and it might be related to the differences in the amount of soil moisture and soil cover between the coastal (mainly devoted to cereal crops) and inland areas of the basin (fruit trees and vegetable crops). After sunrise, the specific humidity increases (about 0.002 kg kg^{-1}) in all locations in the Campos basin but specially in those close to the coastline where this increase is slightly larger. This might be related to the moist evaporation from the soil. Finally, once the SB is established, the specific humidity remains nearly constant everywhere in the basin. There seems to be an equilibrium between the moisture evaporation due to the solar surface heating and the advection of the sea moisture by the SB.

The temperature profiles obtained by the tethered balloon and the multicopter are discussed together with the model outputs in the next section.

2.4. The model setup

To supplement the observations made during the studied MT case, a numerical simulation is performed using the MesoNH model (Lafore et al., 1998). The MesoNH model successfully simulates the SB cycle, as also shown by Talbot et al. (2007) and it has been used by the authors to study the flow at lower levels in the island of Mallorca and in other basins such as the Duero (Martínez et al., 2010), the Ebro (Cuxart and Jiménez, 2012) or the Pyrenees (Jiménez and Cuxart, 2014).

The model setup is identical to the one used in CJTG14. Two nested domains are taken. The outer one (at 5 km $\times$ 5 km horizontal resolution, Figure 1a) covers the Balearic Archipelago whereas the inner one (at 1 km $\times$ 1 km horizontal resolution, Figure 1b) covers Mallorca. A vertical resolution of 3 m is taken close to the surface and is slowly stretched upwards.

The simulation is run for 24 h starting at 1200 UTC of September 19, 2013. Initial and lateral boundary conditions are taken from the ECMWF analyses, refreshed every 6 hours. As in CJTG14, the computation of the temperature, Turbulence Kinetic Energy (TKE) and momentum budgets are activated to allow a substantiated study of the physical processes taking place during the MT.

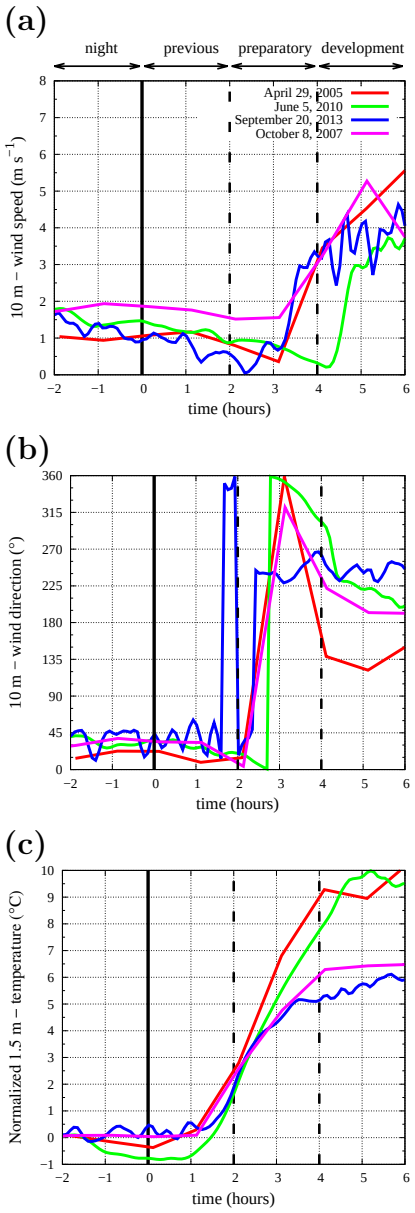

Figure 3: Time series obtained in Ses Salines (see location in Fig. 1) for different simulated cases with a similar setup and under sea-breeze conditions for: **(a)** 10m-wind speed (in m s^{-1}), **(b)** 10m-wind direction (in °) and **(c)** normalized 1.5 m - temperature parameter (in °C) computed as T(t)-T$_{ini}$ being T(t) the temperature at any instant t and T$_{ini}$ the one 2 hours before sunrise for each of the run. The x-axis is normalized by the sunrise time (negative values correspond to hours before sunrise and the positive ones are hours after sunrise). The black vertical line indicates sunrise and those dotted the phases during the morning transition of the SB.

In order to see how representative the present case is, the evolution of the 1.5m-temperature and 10m-wind is compared to the ones of other simulations made for the same area that included a MT in Figure 3. All evolutions - plotted in reference to the sunrise time- are very similar. About 2-3 hours after sunrise the wind veers from N-NE towards S-SW, corresponding to the LB to SB conditions in the Campos basin, meanwhile the temperature warms up. The temperature has been normalized by T_{ini}, corresponding to the temperature 2 hours before sunrise. The amplitude of the diurnal cycle depends on the time of the year (the amount of solar radiation) and the case in June is the one with the largest temperature amplitude. Observations for each of these runs (not shown) agree with these patterns. Figure 3 allows us to consider the present case as representative of a MT between LB and SB. Besides, it strengths that the classification of the SB stages in CJTG14, and specially those during the MT, can be based on sunrise time since all the simulated cases shown in Figure 3 have the same patterns (i.e. time and duration of the warming and wind veering).

3. The modelled flow

3.1. The modelled patterns at lower levels

The modelled patterns during the morning transition between the LB and SB in the Campos basin are shown in Figure 4 where the 10m-wind and 1.5 m temperature are plotted for times corresponding to the relevant periods of the LB (0500 UTC), the MT (0700 UTC, corresponding to the phase previous to the SB, and 0900 UTC, the preparatory phase) and the SB development (at 1100 UTC). This classification is based on the organization of the flow at a basin scale and the precise times of the different SB phases depends on the sunrise time.

The SB is present in the island from late spring to early autumn, and some examples of previous studies are given and Figure 3. The LB may take place along all year. Therefore the MT that is analyzed here can be considered an example of a transition case in the warm period of the year. Figure 3 also illustrates that the defined phases can be seen consecutively in changes in the temperature (for the previous phase), the wind direction (in the preparatory phase) and in the wind speed (in the development phase). The focus is put here on a deeper analysis of the phases during the MT.

The *LB* plots (0500 UTC) indicate the presence of downslope flows over the topography surrounding the flat inner area of the Campos basin, where

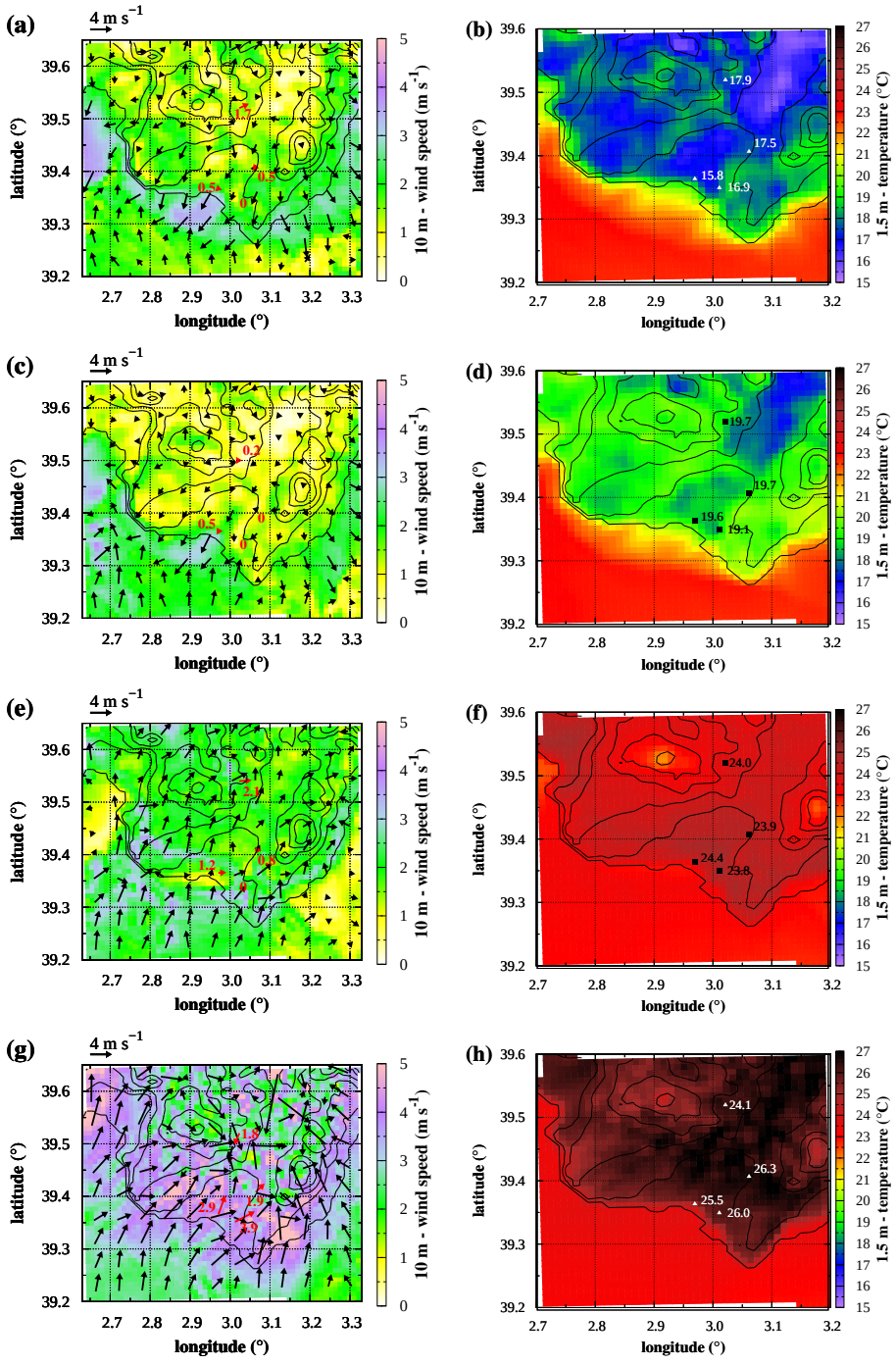

Figure 4: Modelled horizontal cross-sections for the Campos basin on September 20, 2013 for **(a)** 10m-wind direction (black arrows) and speed (in colours) together with the topography (black lines) at 0500 UTC. The numbers and arrows in red indicate the surface observations at this instant. The same in **(b)** but for the 1.5m-temperature (in colours) with the observed values in black and white. The same in **(c)** and **(d)** at 0700 UTC, in **(e)** and **(f)** at 0900 UTC and in **(g)** and **(h)** at 1100 UTC.

the flow is directed outland with cold air flowing over the sea near the coast. The coldest air is over the lowlands and the area in the sea affected by the cold outflow has lower air temperature values (about 2 °C) than the immediate sea areas not reached by the LB. The model is able to capture this spatial temperature gradient although it is smaller than the observed one because it is not reproducing the accumulation of cold air in Ses Covetes due to an excess of mixing. Furthermore, the model is not reproducing the observed spatial variability of the 1.5 m specific humidity reported at different locations in the Campos basin. This might be related to the fact that the spatial heterogeneity of the soil moisture and vegetation cover are poorly represented in the model (at 1 km $\times$ 1 km resolution) similar to what is described in Cuxart et al. (2015). The simulated organization of the flow agrees with data (Figure 2 and Figures 4a and 4b). In Ses Covetes, the model tends to slightly overestimate the wind speed and to provide less variability in direction in comparison with observations, nevertheless it captures the main characteristics of the nocturnal regime, also for temperature and humidity (Figure 2).

During the *previous phase* (0600 - 0800 UTC) wind speed in the Campos basin is still weak and with the LB or downslope directions meanwhile the solar heating warms the land and the specific humidity increases (Figure 2) due to the evaporation from the surface. The strength of the downslope winds decreases (Figure 4c) as the temperature difference between the slope and the center of the basin tends to zero (the ground temperature of the slope and the one at about 400 m agl over the center of the basin are about 294 K, not shown). Although the land surface temperature is warmer than in the previous phase (Figures 4b and 4d), in the center of the basin it is still colder than the one over the sea (Figure 4d). Thus, LB winds are still present in the coastal region (Figure 4c) but less intense than in the previous phase because the thermal difference between land-sea is reduced as well as the strength of the downslope winds during this stage. The model results indicate that downslope winds decrease faster than LB winds, in agreement with the ground observations (Figures 4c and 4d).

The radiative heating of the land continues during the *preparatory phase* (0800 - 1000 UTC) as it is seen from Figure 2 meanwhile the surface temperature over the land becomes warmer than the one over the sea (about 1 K at 0900 UTC, Figure 4f). Therefore the SB is initiated in the coastal region (Figures 2 and 4e) and its strength increases as time (radiative heating) advances. The air in contact with the slopes warms faster than the one in

the center of the basin (thermal difference of about 1 K at 0900 UTC, not shown) favouring the formation of upslope winds. The upslope winds in the mountains at the east side of the Campos basin are strong enough to blow uphill, surpassing the ridges and imposing downslope direction in the east coast. Similarly, there is a combined effect of upslope winds and SB at the south side of the mountain range at the west of the Campos basin and they blow uphill the mountain generating downslope winds in the north side of the mountain range (Figure 4e).

Finally, during the *developing phase* (1000 - 1200 UTC) the wind speed and direction, the temperature and the humidity (Figure 2) remain constant. The land surface temperature is warmer than the sea and this thermal difference is the responsible of the progressing of the SB inland through the lowlands, enhanced by the upslope winds (Figure 4g). The location of the SB front is clearly indicated in pink in Figure 4g at about 15 km from the coast to the inland direction at 1100 UTC (the progress of the SB front is about 15 km in 2 hours, corresponding to an approximate speed of the breeze front of 2 m s^{-1}). In complex terrain regions, as the Campos basin, upslope winds interact with SB, as it is described in Papanastasiou et al. (2010) for the east coast of Greece. Regarding the temperature, during the developing phase the 1.5m-temperature levels off (Figure 2) because the SB favours the advection of cold air from the sea over the land. As a result, the ground temperature in the coastal region over the land is colder than further inland (Figure 4h) where it is nearly homogeneous. Observations agree with the model results, as it is indicated in Figures 2, 4g and 4h.

3.2. The vertical structure of the simulated flow

Vertical cross-sections along a line through the central part of the Campos basin and perpendicular to the coastline (Figure 1c) are shown in Figure 5 for the wind and potential temperature. In the LB period, the wind flows outland (corresponding to the NE direction, in blue in Figure 5a) for a distance near 12 km, with a depth slightly above 100 m, speeds between 3 and 4 m s^{-1} with maximal values near 50 m agl. Unstably stratified conditions are found in the surface layer over the sea (Figure 5b) due to the cold advection present under LB conditions. Over land, downslope winds are found at the slopes with wind maxima weaker (about 2-3 m s^{-1}) and lower (about 30 m agl) than the ones related to the LB. Besides, downslope winds flow over the surface thermal inversion enhancing the transport of cold air over the sea.

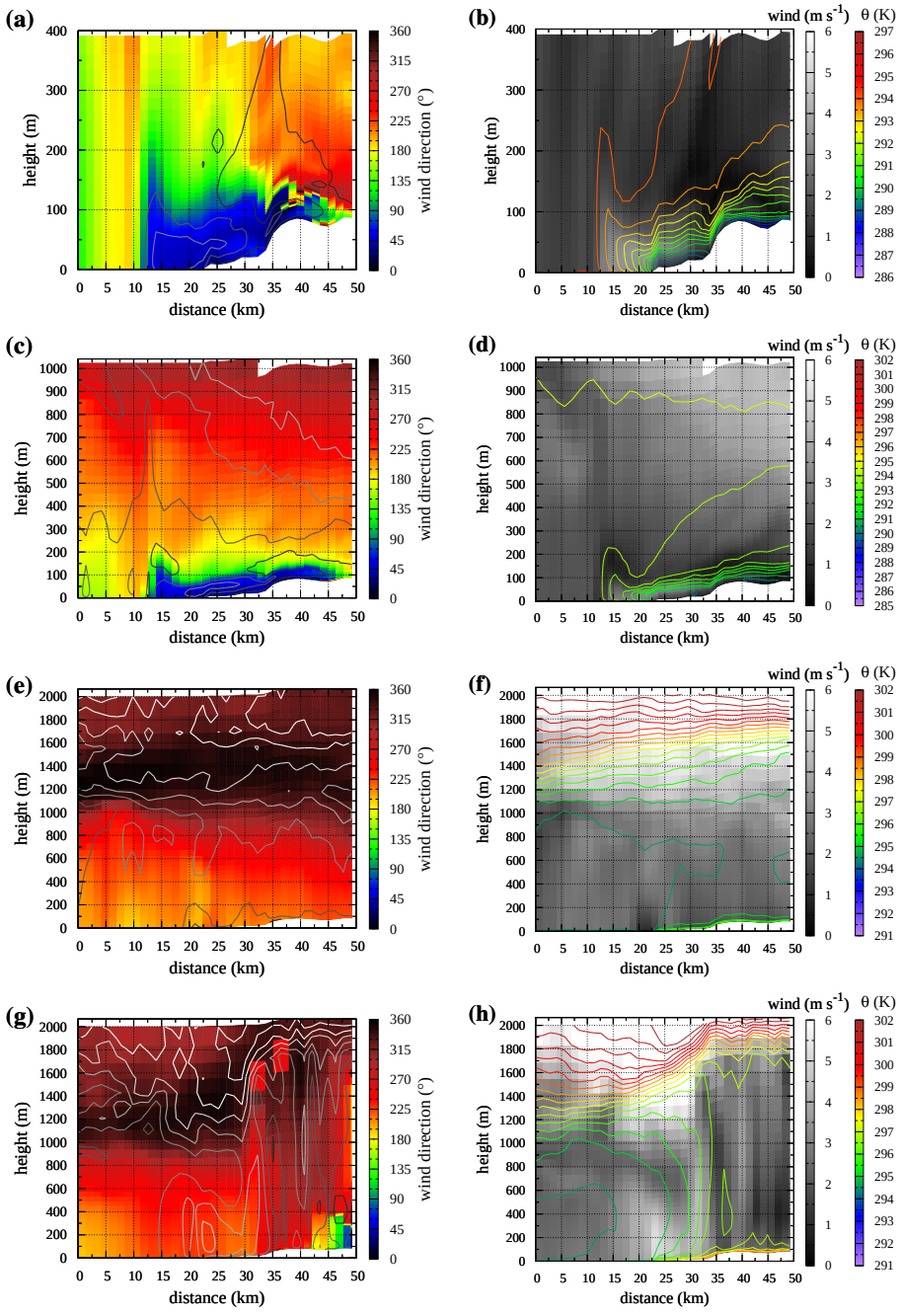

Figure 5: Modeled vertical cross-sections along the black line in Figure 1 for different instants on September 20, 2013. **(a)** Wind direction (in colours) and speed (in black and white lines every 1 m s^{-1}) and **(b)** wind speed (in black and white) and potential temperature (in coloured lines every 0.5 K) at 0500 UTC (LB phase). The same in **(c)** and **(d)**, **(e)** and **(f)** and **(g)** and **(h)** at 0700 UTC (previous phase), 0900 UTC (preparatory phase) and 1100 UTC (development phase), respectively. For **(a)**-**(b)** the vertical profiles are shown up to 400 m (asl), for **(c)**-**(d)** up to 1000 m (asl) and for **(e)**-**(h)** up to 2000 m (asl) to include the whole boundary layer extend. The colour scale of the temperature changes for the different phases to better show the boundary layer extend.

In the previous phase (0600 - 0800 UTC), already under the sunlight, the structures keep the same shapes as the ones on the LB, but progressively weakening. The horizontal extent of the LB over the sea diminishes and the outflow vertically shrinks, while the regime is still unstable over the sea and stable over the land (Figures 5c and 5d).

The preparatory phase (Figures 5e and 5f) indicates that the outland wind has vanished -although there is still an area of minimal wind speed offshore where the end of the LB flow was- and there is the establishment of a local wind maximum over the shore, still not progressing inland. A well mixed convective boundary layer is found and neutral stratification prevails over land and sea with an homogeneous temperature of about 295 K up to 1000 m above sea level (asl). Over the land, the surface layer becomes unstable due to the radiative heating of the terrain.

This heating causes that during the development phase (Figures 5g and 5h) an horizontal thermal gradient between the air over land and sea is found at 1100 UTC (2.5 K in 20 km). The cold air flows over a heated land (unstably stratified conditions in the surface layer) along this horizontal temperature gradient and a maximum of wind related to the SB direction (SW) is found (wind speed reaches values of 6 m s^{-1} over a depth of 400 m). Further inland (distances 35-50 km in Figure 5g) the convective boundary layer grows due to the radiative heating of the ground without any horizontal advection of cold air due to the SB resulting in a height of 1600 m agl (Figure 5h) larger than the one in the coastal region. Besides, winds are weaker than those related to the SB and from NW (Figure 4g), indicating that the SB front has still not reached this region.

3.3. Thermal structure during the MT

The surface weather stations in the basin, as well as the surface observations in Ses Covetes, are used to validate the model results (see Figures 2 and 4). Furthermore, the observed vertical profiles of temperature in the lower atmosphere taken during MSB13 allow us to verify the modelled thermal profiles in the lower atmosphere in Ses Covetes.

The time evolution of the temperature profile in Ses Covetes as observed by the multicopter is plotted in Figure 6a and compared to the corresponding field extracted from the model (Figure 6b). The modelled wind speed and direction are also included in the plot (Figures 6c and 6d) although these magnitudes are not measured along the lower atmosphere. Furthermore, Figure 7 compares time-averaged values for the different phases from the

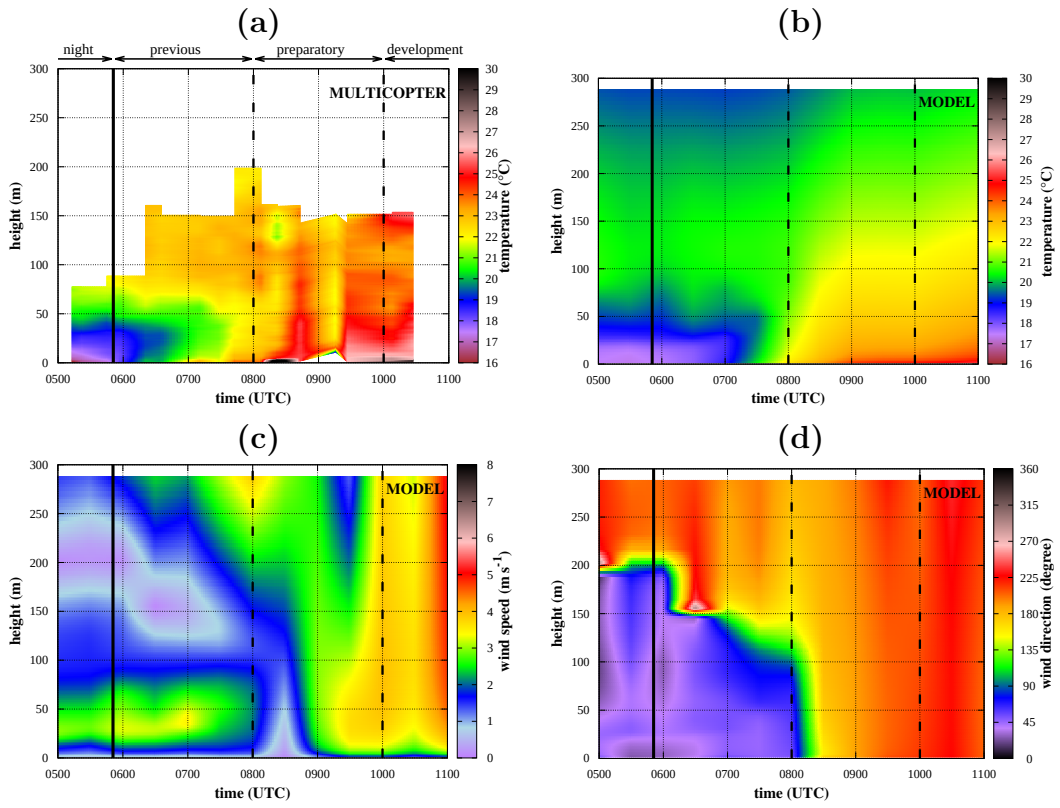

Figure 6: Time evolution of the vertical profiles in Ses Covetes during the morning transition on September 20, 2013 for **(a)** temperature observed by the multicopter and the model results for **(b)** temperature, **(c)** wind speed and **(d)** wind direction. The black vertical line indicates the sunrise time and the dotted ones the different phases during the morning transition (names in **(a)**).

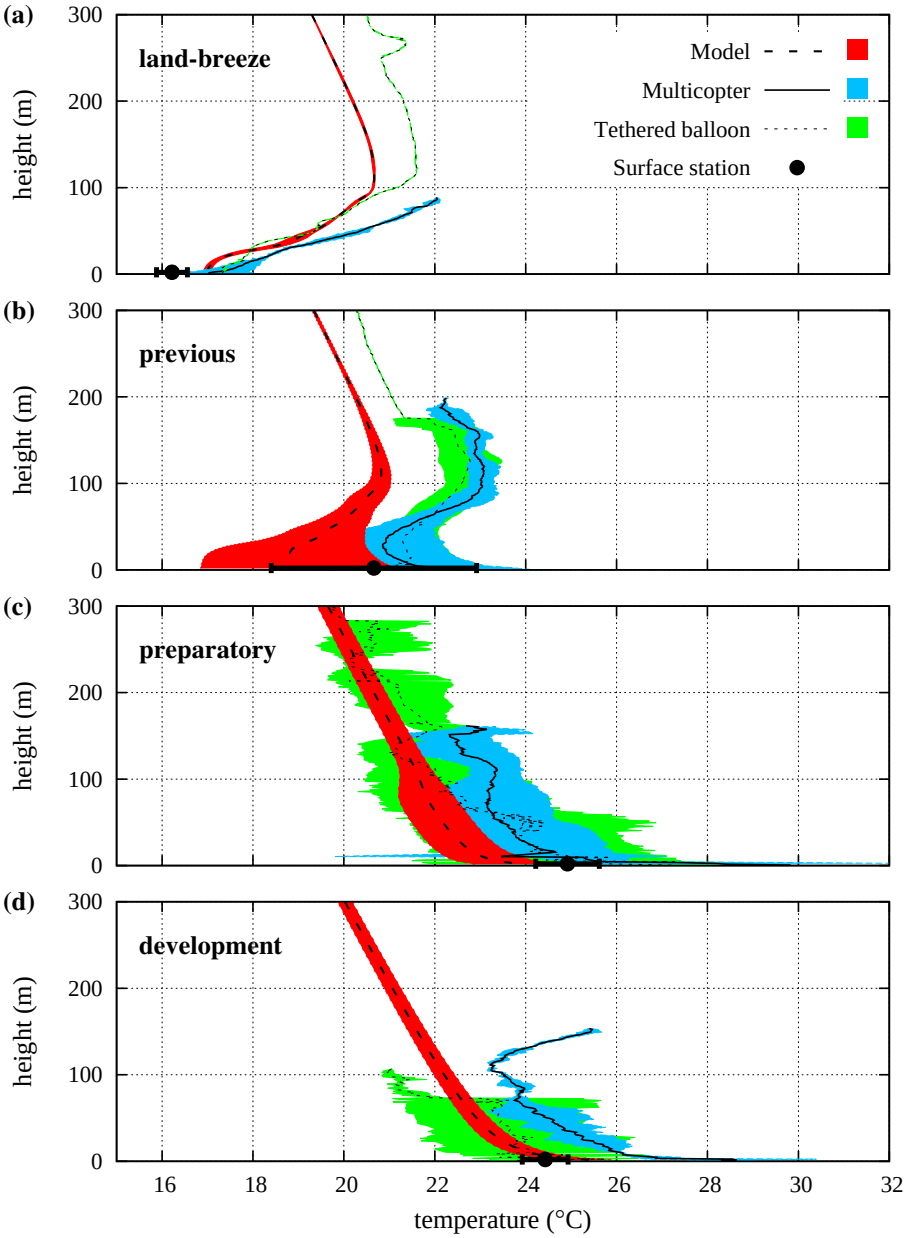

Figure 7: Vertical profiles in Ses Covetes measured by the multicopter (solid line) and tethered balloon (dotted line) together with those obtained from the MesoNH model (dashed line). The corresponding value measured by the surface station at 2 m agl is also included (mean value with a dot and the standard deviation with error bars). The profiles are averaged over the different phases during the morning transition of September 20, 2013: **(a)** night-time (0500 - 0600 UTC), **(b)** previous (0600 - 0800 UTC), **(c)** preparatory (0800 - 1000 UTC) and **(d)** development (1000 - 1200 UTC). The mean values are indicated with a line and the colours indicate the standard deviation.

model, the multicopter, the tethered balloon and the surface observations at the site.

During the *LB phase* in Ses Covetes, a surface thermal inversion up to about 50-70 m agl is found for the model and observations (Figures 6a and 6b) although the observed surface layer is more stably stratified than the one simulated (see Figure 7a). From the model results it is found that in the first 200 m agl, there is a layer of NE winds (Figure 6d, corresponding to LB direction) with maximum speeds of 2-3 m s^{-1} at about 40 m agl (Figure 6c). The averaged observed and modelled thermal profiles during this phase (from 0500 to 0600 UTC, Figure 7a) are very similar, indicating a thermal inversion up to 100 m. In the surface layer, the model mixes in excess compared to observations, a fact known from long as a default particular for this model and some similar ones (Bravo et al., 2008).

After sunrise, the solar radiative warming of the ground is responsible for the increase of the 1.5m-temperature. The modeled and observed 1.5m-temperatures are similar at the end of the *previous phase* although at the beginning, the observed one was colder than the modelled one (Ses Covetes, Figure 2). The progressive warming explains the large value of standard deviation of the averaged modelled and observed temperatures during this phase (Figure 7b). Nevertheless, at the end of the previous phase (0800 UTC) both temperatures are similar although their temporal evolution along this phase somewhat differ (Figure 6a and 6b) being the averaged modelled temperatures colder than those observed (Figure 7b). Observations (Figure 6a) show that the solar radiative warming starts close to the surface (at about 10 m agl) and the heat is transported upwards. This is not captured by the model (Figure 6b) where the whole boundary layer depth warms up just after the LB weakens (Figures 6c and 6d). Transitions are the most difficult part of the diurnal cycle for the models to reproduce adequately (Lothon et al., 2014).

During the *preparatory phase* the warming of the surface layer continues but at a lower rate (Figure 2). The temperature in the lower atmosphere continues increasing and a cooling event is reported between 0900-0930 UTC (Figure 6a). The model is not able to capture this event although at this time the temperature in the lower atmosphere levels off (Figure 6b), the wind speed increases (Figure 6c) and the wind direction corresponds to the SB (Figure 6d). As in the previous phase, probably the strong mixing in the model is the responsible of not capturing the cooling event related to the arrival of the SB front in Ses Covetes. The observed and modelled averaged

vertical profiles (Figure 7c) are similar although the standard deviation in the observed ones is larger than on the simulated ones where the cooling related to the arrival of the SB is not captured.

Finally, the averaged thermal structure in the model during the *development phase* is similar to the one measured by tethered balloon (Figure 7d). The differences of the temperature values in this phase between the multicopter and tethered balloon may be in the different response of each device to the effect of the solar radiation. Nevertheless, model and observations are producing a well-mixed boundary layer meanwhile the wind increases intensity (Figure 6c) and remains from the SB direction (Figure 6d). A temperature inversion is reported by the multicopter at about 120 m agl (Figure 7d), but this may be related to its sampling of a turbulent eddy, a feature not captured by the model

Figure 7 shows that the model is able to capture the observed temperature profile during the different phases of the MT, except for the temporal evolution during the previous phase, when LB is still present but the solar radiative warming starts. These differences might be related to a poor representation in the model of the physical processes that take place there, specially those related to the interaction between the land and atmosphere. Besides, if the surface parameters (such as the soil moisture) are far from the real ones, the modelled surface fluxes can depart very much from the observed ones, as it is shown in Cuxart et al. (2015).

4. Temperature and turbulence budgets

Similarly to the analysis made in CJTG14, the budgets of temperature and TKE are discussed for this case. Figure 8 displays the spatial distribution of these budgets along the line normal to the coast (Figure 1) for the different phases during the MT, averaged for one hour. Here the attention is focused on the evolution of these budgets during the MT in the coastal zone (land and sea) whereas in CJTG14 a deeper discussion during the mature phase of the SB over land is found.

The temperature budget clearly indicates that in all phases except in the preparatory phase (land warming but the SB already not blowing) the main process is the advection by the LB or the SB respectively, and the main response is the turbulence mixing, that redistributes vertically the heat as necessary. A key mechanism keeping the system going is the radiation heating of the lower layers of the air over the sea at night and over the land

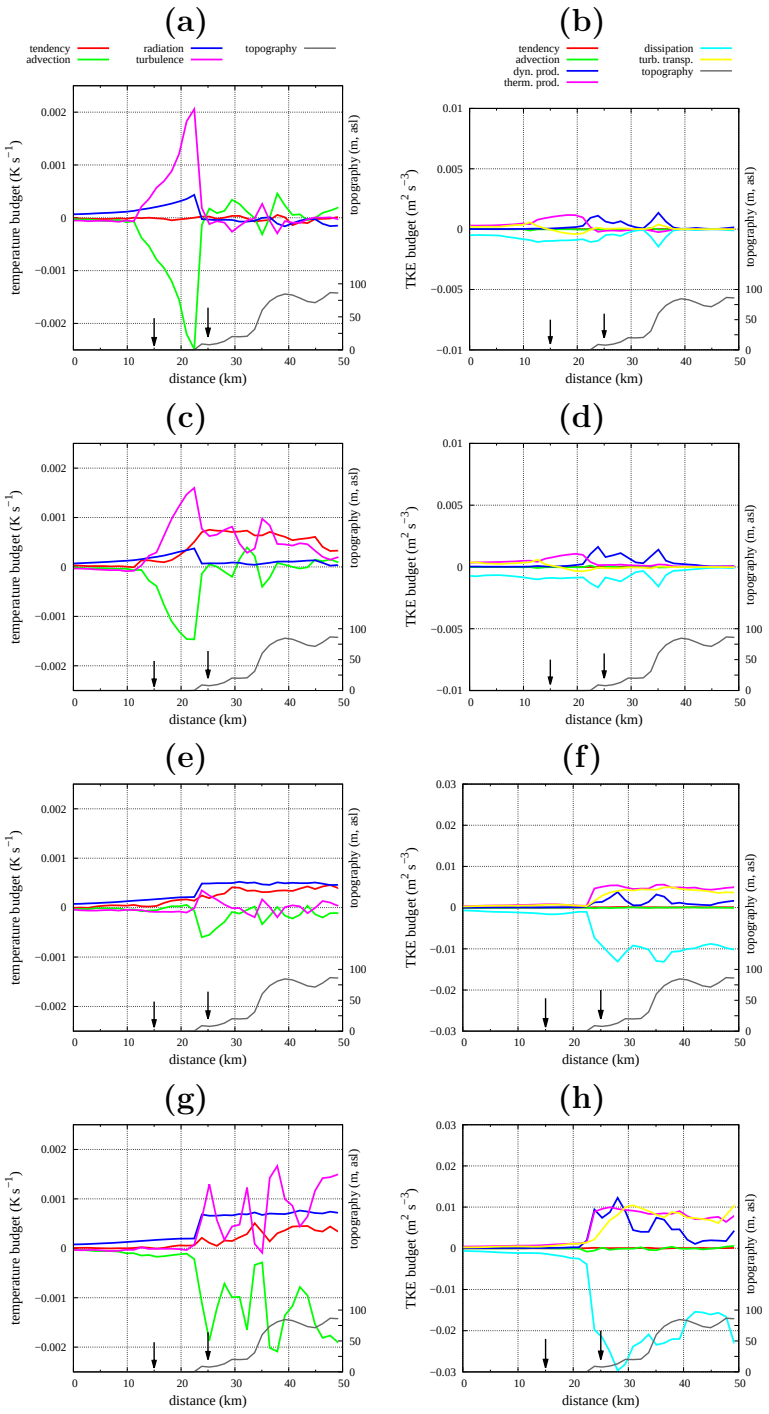

Figure 8: Temperature and TKE budgets at 10 m agl along a line normal to the coast (see location in Figure 1) averaged over 1 hour and at different instants: **(a)** and **(b)** nighttime (0430-0530 UTC); **(c)** and **(d)** previous (0630-0730 UTC); **(e)** and **(f)** preparatory (0830-0930 UTC) and **(g)** and **(h)** development (1000-1100 UTC). The arrows indicate the location of the vertical profile budgets shown in Figure 9. For the TKE budgets the y-axis is changed in **(f)** and **(h)** to clearly see the patterns during the different SB phases.

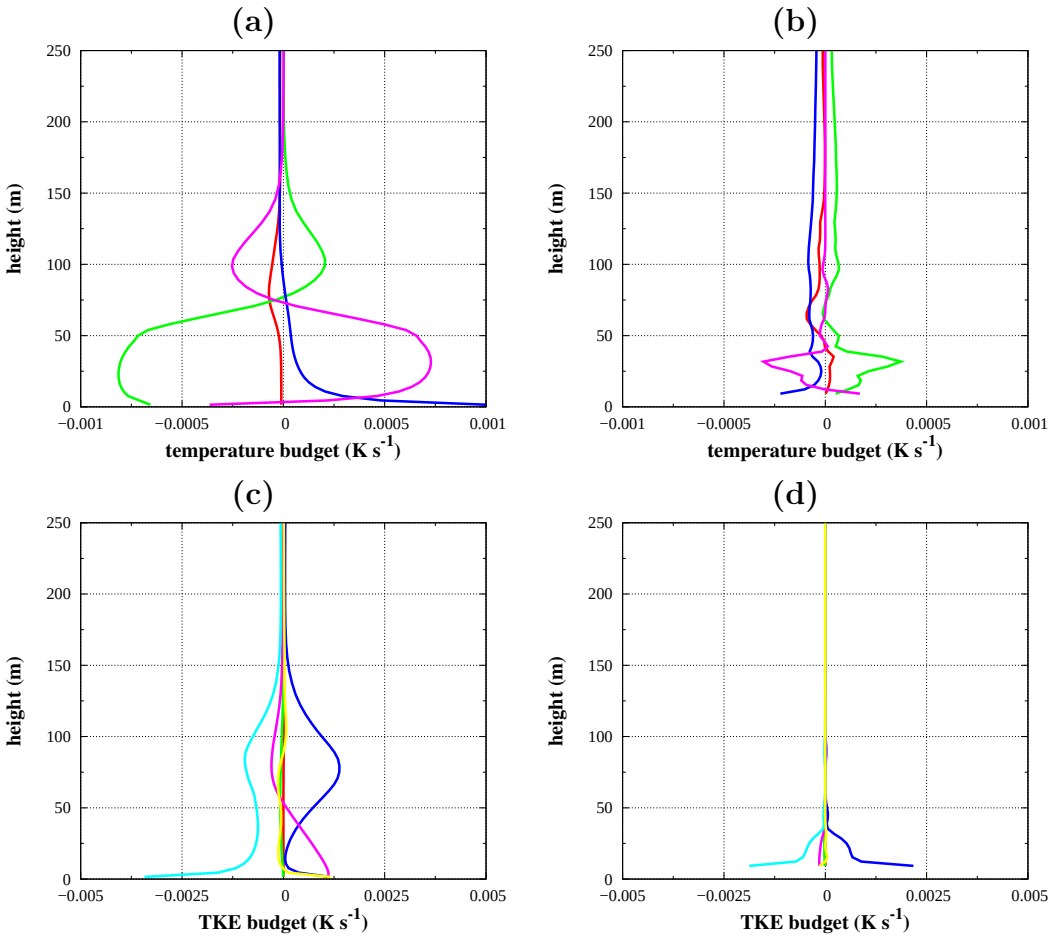

Figure 9: Temperature budget averaged between 0430 - 0530 UTC for a point **(a)** 6.5 km offshore and **(b)** 3.5 km inland, respectively. The same in **(c)** and **(d)** for the TKE budget. The location of these points and the colours of the lines are explained in Figure 8.

in the daytime, especially in the preparatory and developing phases over land, periods during which there is a clear warming tendency over the latter.

The momentum budget (not shown) indicates that the main driving factor is the pressure gradient term, that results from having different densities at both sides of the coastline. The response is an advection of momentum, delayed by the turbulent mixing, mechanisms that are active in all phases, except in the preparatory one.

The TKE budget terms are very weak in the LB and the previous phase but they are stronger for the preparatory and development phases (Figure 8). In the preparatory phase (Figure 8f), the surface heating over land results in the predominance of the thermal production of turbulence and the resulting vertical transport of it, with local circulations associated that produce dynamically some extra turbulence. In the development phase (Figure 8h), the inflow produces, through shear production, as much TKE as the surface heating, and this excess of turbulence is transported upwards by the turbulence transport.

The vertical structure of the budgets during the LB phase (those during the mature phase are found in CJTG14) are further inspected in Figure 9, averaged over 1 hour for one point over the sea (left column) and over the land (right column).

The budgets show more activity over the sea where, according to the temperature budget, the radiative warming by the sea surface of the lowest layers of air is transported upwards up to 120 m agl by the turbulence. The TKE budget shows that thermal production of turbulence dominates near the surface and that the dynamic production prevails above, where the speed gradients are largest.

Over land radiation cools near the surface and turbulence diffuses this cooling upwards compensated by a slight warming advection of the katabatic flow warmed by adiabatic compression, but all these processes are much smaller in magnitude than over the sea, and extend only up to 50 m agl at most. The production of turbulence is only through the wind shear close to the surface, significant but very shallow as well.

It is noteworthy that the budgets during the LB are qualitatively inverted in respect those of the mature phase, where the main activity takes place over the land.

5. Sensitivity to the minimum value of TKE in the turbulence scheme

It is a well known feature of the numerical models that are run with a TKE turbulence scheme, such as Meso-NH (Lafore et al. (1998); Cuxart et al. (2000)), that they have one adjustable parameter, which is the minimum value allowed for the TKE (TKEMIN) in case of no turbulence present. In the model, the cold surface may decouple from the warmer air above, leading to unrealistic near-the-surface temperature values (the *runaway cooling* problem, as introduced by Viterbo et al. (1999)). Some models take a minimum value of the order of 0.1 $m^2\ s^{-2}$, large compared to the average values of a calm night (Cuxart and Jiménez, 2012). This way they ensure mixing, even if there is in reality no turbulence performing it and other processes are acting. Comparing the observed and modelled temperature profiles (Figure 7) it is found that in the surface layer the model produced large turbulent mixing and the observed strong surface inversion in Ses Covetes is not captured by the model.

In our study above we have used a TKEMIN of 10^{-5} $m^2\ s^{-2}$ (our standard run), which is well below the minimum observed values in stably stratified conditions. We have made another simulation with the default value in MesoNH (10^{-2} $m^2\ s^{-2}$), to see what is the sensitivity of the model to this change, but without altering excessively the physical mechanisms as it would happen imposing an even larger minimal value.

Figure 10 summarizes some of the changes that take place in this exercise. The upper frames show that in the sites of Ses Covetes and Porreres the values at 10 m of TKE do not change significantly, but there are some evident differences in the vertically integrated values, especially in Ses Covetes where a cold pool is formed and turbulence is minimal. There, during the second part of the night and the early morning transition, when the lower TKEMIN manages to sustain a more turbulent regime than the artificially-increased one, and delays for some hours the establishment of a developed convective boundary layer over the site.

Looking at the profiles we see that the change of TKEMIN does not change much the direction or the wind speed of the lower layers of the LB, but has an appreciable effect on the layer above the jet. Our standard run has a softer transition between the jet and the slower air above, which allows the TKE to have significant values in that layer. The effects of this change in the integrated TKE value, which is larger for the default TKEMIN (10^{-2}

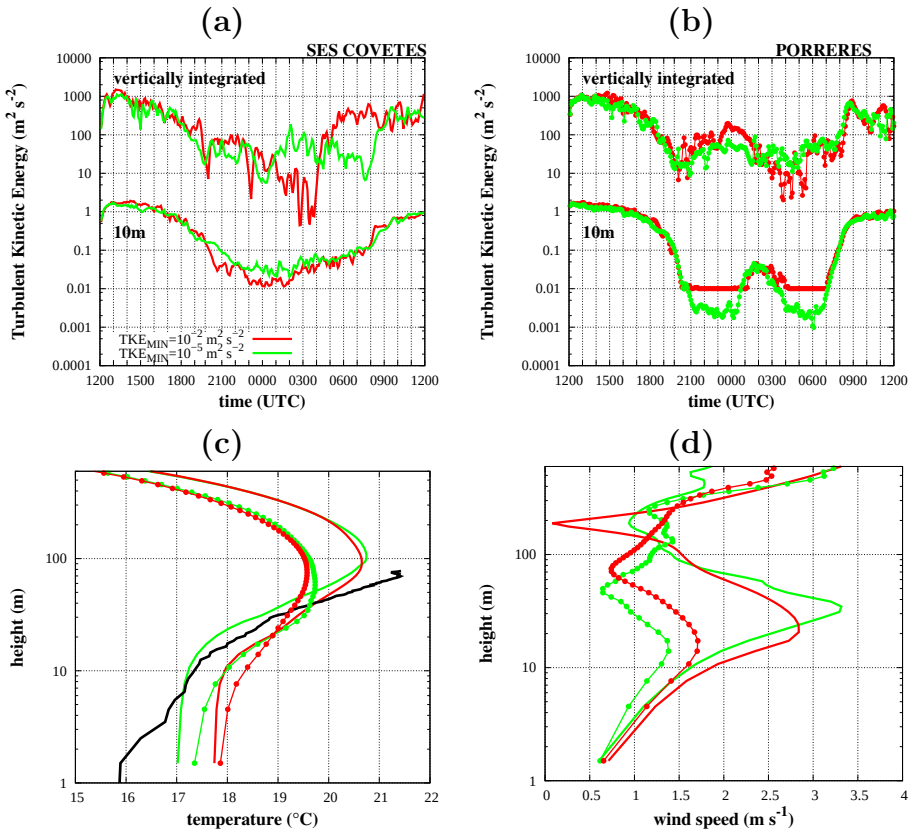

Figure 10: Temporal evolution of the 10 m (agl) TKE and the vertically integrated TKE over the first 1 km for **(a)** Ses Salines and **(b)** Porreres (see locations in Figure 1). In red the run with default TKE_{min} and in green the one with reduced TKE_{min}. In **(c)** and **(d)** there are the profiles of the temperature and wind speed at 0500 UTC for the same locations and runs (the same color and lines as in **(a)** and **(b)**). The multicopter observations at 0500 UTC are also shown with a black line.

$m^2\ s^{-2}$) is that it allows for a more efficient transport upwards of the cold air at the surface and the resulting surface layer is colder and better mixed than the case with larger TKEMIN. Besides, the observed temperature profile in Figure 10c indicates that once the TKEMIN is reduced, the modelled surface layer is closer to the observations, specially in Ses Covetes.

Similar results (Figures 10c and 10d) are found for the previous phase but for the rest of the MT phase, there are not significant differences in the profiles between the default and reduced TKEMIN.

6. Conclusions

This work has analyzed a morning transition (MT) case between the land-breeze (LB) and the sea-breeze (SB) regimes taking advantage of the data gathered during an experimental campaign near the seashore, that has been used to check the performance of the numerical simulation of the case. The transition between LB and SB is seen to happen in four distinct steps, according to the observed temporal evolution of the wind and temperature in the lower atmosphere.

It is found that for all the different phases during the MT the model is able to capture the organization of the flow at lower levels. Nevertheless, the cold pool formed at the center of the basin during the LB seen by the model is about 1-2 K warmer than the observed one probably due to a too strong turbulent mixing in the model. The model is not able to capture adequately the temporal evolution of the thermal profile, showing that the morning transition, when the model energy budget usually differs a lot from the observed one, is a difficult regime for the physics of the model. This might be related to a wrong representation of the surface layer processes and an unrealistic surface properties (soil moisture or surface cover). Nevertheless, at the end of this phase the model agrees with the observations, showing that the general energetics of the MT are well captured. A sensitivity test on the imposed minimum value of the TKE in the turbulence scheme of the model shows that the most realistic model results are the ones with the reduced value.

The representation of the MT by the model is, in general, satisfactory, although an improvement of the morning heating of the surface would be needed and this issue must be further investigated, for instance comparing the modelled and measured surface energy budgets. There is a sustained lack of observational information over the sea that limits the capacity of

interpretation of the coastal processes since verification is scarce in that area. The availability of vertical profiles of temperature and humidity has allowed to analyze in depth the evolution of the MT and it should be supplemented with wind profiles at both sides of the coast line. It has also been shown that the models results are sensitive to relatively minor changes in their choices and that extreme caution must be taken when defining the simulation setup. Finally, it is expected that future higher horizontal resolution simulations may provide a finer description of the processes at the coastal area.

Acknowledgements A. Burguera and A. Fullana are acknowledged for letting us employ their field to perform our measurements, and the students M. Ponsetí and B. Martí for helping us in the field. ECMWF and AEMET are thanked for the access to computing time and the Meso-NH team in Meteo France and Laboratoire d'Aérologie for their support. This work was funded through the projects CGL2009-12797-C03-01 and CGL2012-37416-C04-01 of the Spanish Government, supplied by the European Regional Development Fund (FEDER), and M.A. Jiménez with a contract JAE-Doc of the *Junta para la Ampliación de Estudios* program from CSIC supplied by the European Social Fund.

References

Atkinson, B. W., 1981. Meso-scale Atmospheric Circulations. Academic Press.

Azorin-Molina, C., Chen, D., 2009. A climatological study of the influence of synoptic-scale flows on sea breeze evolution in the Bay of Alicante (Spain). Theoretical and Applied Climatology 96, 249–260.

Azorin-Molina, C., Tijm, S., Ebert, E. E., Vicente-Serrano, S. M., Estrela, M. J., 2014. Sea breeze thunderstorms in the eastern iberian peninsula. neighborhood verification of HIRLAM and HARMONIE precipitation forecasts. Atmos. Res. 139, 101–115.

Bechtold, P., Pinty, J.-P., Mascart, P., 1991. A numerical investigation of the influence of large-scale winds on sea-breeze- and inland-breeze-type circulations. J. Appl. Meteor. 30, 1268–1279.

574 Bravo, M., Mira, T., Soler, M. R., Cuxart, J., 2008. Intercomparison and
575 evaluation of mm5 and meso-nh mesoscale models in the stable boundary
576 layer. Boundary-Layer Meteorology 128, 77–101.

577 Cuxart, J., Bougeault, P., Redelsperger, J.-L., 2000. A turbulence scheme
578 allowing for mesoscale and large-eddy simulations. Quart. J. Roy. Meteor.
579 Soc. 126, 1–30.

580 Cuxart, J., Conangla, L., Jiménez, M. A., 2015. Evaluation of the surface
581 energy budget equation with experimental data and the ECMWF model
582 in the Ebro Valley. J. Geophys. Res. Atmos. 120, 1008–1022.

583 Cuxart, J., Jiménez, M. A., 2007. Mixing processes in a nocturnal low-level
584 jet: An les study. J. Atmos. Sci. 64, 1666–1679.

585 Cuxart, J., Jiménez, M. A., 2012. Deep radiation fog in a wide closed val-
586 ley: study by numerical modeling and remote sensing. Pure and Applied
587 Geophysics 169, 911–926.

588 Cuxart, J., Jiménez, M. A., Martínez, D., 2007. Nocturnal meso-beta basin
589 and katabatic flows on a midlatitude island. Mon. Wea. Rev. 135, 918–932.

590 Cuxart, J., Jiménez, M. A., Telisman-Prtenjak, M., Grisogono, B., 2014.
591 Study of a sea-breeze case through momentum, temperature, and turbu-
592 lence budgets. J. Appl. Meteor. Climatol. 53, 2589–2609.

593 Garratt, J. R., 1992. The atmospheric boundary layer. Cambridge University
594 Press.

595 Jansà, J. M., Jaume, E., 1946. The sea breeze regime in the Mallorca island
596 (in Spanish). Rev. Geofis. 19, 304–328.

597 Jiménez, M. A., Cuxart, J., 2014. A study of the nocturnal flows generated
598 in the north side of the Pyrenees. Atmos. Res. 145–146, 244–254.

599 Jiménez, M. A., Cuxart, J., Mira, A., Martínez, D., 2006. Local nocturnal
600 circulations in the island of Majorca: mesoscale modelling and verification.
601 Tethys 3, 67–73.

602 Johnson, A., O'Brien, J. J., 1973. A study of an Oregon sea breeze event. J.
603 Appl. Meteor. 12, 1267–1283.

Lafore, J. P., Stein, J., Asencio, N., Bougeault, P., Ducrocq, V., Duron, J., Fisher, C., Héreil, P., Mascart, P., Pinty, J.-P., Redelsperger, J.-L., Richard, E., de Arellano, J. V.-G., 1998. The Meso-NH atmospheric simulation system. Part I: Adiabatic formulation and control simulation. Ann. Geophys. 16, 90–109.

Lapworth, A., 2003. Factors determining the decrease in surface wind speed following the evening transition. Q.J.R. Meteorol. Soc. 129, 1945–1968.

Lapworth, A., 2006. The morning transition of the nocturnal boundary layer. Boundary-Layer Meteorology 119, 501–526.

Lenschow, D. H., Stankov, B. B., Mahrt, L., 1979. The rapid morning boundary-layer transition. J. Atmos. Sci. 36, 2108–2124.

Lothon, M., Lohou, F., Pino, D., Couvreux, F., Pardyjak, E. R., Reuder, J., de Arellano, J. V.-G., Durand, P., Hartogensis, O., Legain, D., Augustin, P., Gioli, B., Lenschow, D. H., Faloona, I., Yagüe, C., Alexander, D. C., Angevine, W. M., Bargain, E., Barrié, J., Bazile, E., Bezombes, Y., Blay-Carreras, E., van de Boer, A., Boichard, J. L., Bourdon, A., Butet, A., Campistron, B., de Coster, O., Cuxart, J., Dabas, A., Darbieu, C., Deboudt, K., Delbarre, H., Derrien, S., Flament, P., Fourmentin, M., Garai, A., Gibert, F., Graf, A., Groebner, J., Guichard, F., Jiménez, M. A., Jonassen, M., van den Kroonenberg, A., Magliulo, V., Martin, S., Martínez, D., Mastrorillo, L., Moene, A. F., Molinos, F., Moulin, E., Pietersen, H., Piguet, B., Pique, E., Román-Cascón, C., Rufin-Soler, C., Saïd, F., Sastre-Marugán, M., Seity, Y., Steeneveld, G. J., Toscano, P., Traullé, O., Tzanos, D., Wacker, S., Wildmann, N., Zaldei, A., 2014. The BLLAST field experiment: Boundary-Layer Late Afternoon and Sunset Turbulence. Atmos. Chem. Phys. 14, 10931–10960.

Martínez, D., Jiménez, M. A., Cuxart, J., Mahrt, L., 2010. Heterogeneous nocturnal cooling in a large basin under very stable conditions. Bound.-Layer Meteor. 137, 97–113.

Miao, J. F., Kroon, L. J. M., de Arellano, J. V.-G., Holtslag, A. A. M., 2003. Impacts of topography and land degradation on the sea breeze over eastern Spain. Meteorology and Atmospheric Physics 84, 157–170.

Nadeau, D. F., Pardyjak, E. R., Higgins, C. W., Fernando, H. J. S., Parlange, M. B., 2011. A simple model for the afternoon and early evening decay of convective turbulence over different land surfaces. Boundary-Layer Meteorology 141, 301–324.

Nelci, A., Miglietta, M. M., Rizza, U., Acevedo, O. C., Degrazia, G. A., 2015. Investigation of sea-breeze convergence in Salento Peninsula (southeastern Italy). Atmos. Res. 160, 68–79.

Panchal, N., 1993. Onset characteristics of land/sea breeze circulation and its effect on meterological parameters at a coastal site. Atmósfera 6, 155–162.

Papanastasiou, D. K., Melas, D., Lissaridis, I., 2010. Study of wind field under sea breeze conditions; an application of WRF model. Atmos. Res. 98, 102–117.

Poljak, G., Prtenjak, M. T., Kvakić, M., Mahović, N. S., Babić, K., 2014. Wind patterns associated with the development of daytime thunderstorms over Istria. Ann. Geophys. 32, 401–420.

Ramis, C., Alonso, S., 1998. Sea-breeze convergence line in Majorca: a satellite observation. Weather 43, 288–293.

Ramis, C., Romero, R., 1995. A first numerical simulation of the development and structure of the sea breeze on the island of Mallorca. Ann. Geophys. 13, 981–994.

Sun, J., Mahrt, L., Banta, R. M., Pichugina, Y. L., 2012. Turbulence regimes and turbulence intermittency in the Stable Boundary Layer during CASES-99. J. Atmos. Sci. 69, 338–351.

Talbot, C., Augustin, P., Leroy, C., Willart, V., Delbarre, H., Khomenko, G., 2007. Impact of a sea breeze on the boundary-layer dynamics and the atmospheric stratification in a coastal area of the North Sea. Bound.-Layer Meteor. 125, 133–154.

Telisman-Prtenjak, M., Viher, M., Jurkovic, J., 2010. Sea-land breeze development during a summer bora event along the north-eastern adriatic coast. Q. J. R. Meteorol. Soc. 136, 1554–1571.

Viterbo, P., Beljaars, A. C. M., Mahfouf, J. F., Teixeira, J., 1999. The representation of soil moisture freezing and its impact on the stable boundary layer. Q. J. R. Meteorol. Soc. 125, 2401–2426.

Whiteman, C. D., 2000. Mountain meteorology. Fundamentals and applications. Oxford University Press.